

## RADIUS AND LIMB DARKENING OF TITAN FROM SPECKLE IMAGING

PETER NISENSEN<sup>a)</sup>

Center for Earth and Planetary Physics, Harvard University, Cambridge, Massachusetts 02138

JEROME APT

Jet Propulsion Laboratory, California Institute of Technology, Pasadena, California 91103

RICHARD GOODY<sup>a)</sup>

Center for Earth and Planetary Physics, Harvard University, Cambridge, Massachusetts 02138

PAUL HOROWITZ

Physics Department, Harvard University, Cambridge, Massachusetts 02138

Received 29 June 1981; revised 27 July 1981

## ABSTRACT

We have used a two-dimensional speckle-imaging technique to determine the radius ( $R$ ) of Titan from ground-based visible-light observations. The value of  $R$  depends somewhat upon the limb-darkening exponent ( $\alpha$ ) used to model the observed disk; the probable range extends from  $R = 2680 \pm 100$  km for  $\alpha = 0.6$  to  $R = 2900 \pm 100$  km for  $\alpha = 1.3$ , and is in good agreement with both Voyager 1 and Pioneer Saturn observations.

## I. INTRODUCTION

We have developed a speckle camera and a practical version of the Knox-Thompson algorithm (Knox and Thompson 1974) for restoring atmospherically degraded astronomical images. A description of the technique and the instrumentation is given by Nisenson *et al.* (1980). Here we present results for Titan from which we have been able to determine the radius as a function of the limb darkening of the satellite.

## II. OBSERVATIONS

Images of Titan were recorded with the 2.24-m University of Hawaii telescope on Mauna Kea on 9 July 1980. The intensified video camera described by Nisenson *et al.* (1980) was used at Cassegrain focus with the  $f/10$  secondary, such that the  $128 \times 128$  picture elements (pixels) of each digitized frame corresponded to  $11.2 \times 11.2$  arcsec. 2500 frames of Titan were recorded from 0600–0606 UT with no optical filter, the spectral response being determined by the channel plate intensifier whose sensitivity has fallen to 50% at 340 and 600 nm, respectively. For these observations the exposure time per frame was 4 ms and the zenith angle was  $48.5^\circ$ . 1350 frames of Titan were recorded from 0643–0646 UT through a 425–475-nm filter, with an exposure time of 16 ms per frame and zenith angle of  $58^\circ$ . In order to obtain the spatial response of the system we recorded 225 frames of  $\sigma$  Leo, an unresolved star that does not possess known spectroscopic companions. These comparison data were obtained through the 425–475-nm fil-

ter at 0549 UT on the same date with an exposure time of 4 ms/frame and zenith angle of  $47^\circ$ . The repetition rate for all observations was 7.5 frames/s. The aspect of Titan at the time of our observations is shown in Fig. 1.

## III. DATA REDUCTION

The method of data reduction is described by Nisenson *et al.* (1980). It differs from that of other workers by the use of a practical version of the Knox-Thompson algorithm for phase reconstruction.

The three data sets, recorded on 3/4-in. video tape,

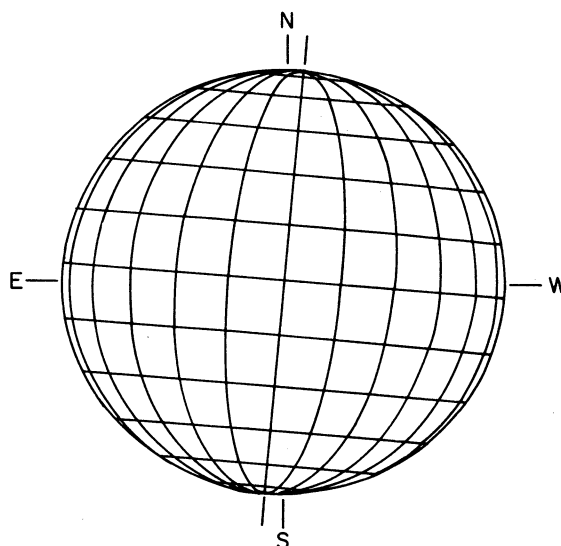


FIG. 1. The aspect of Titan as viewed from Earth at the time of our observations. The pole of Titan's orbit was used in these computations. The sub-Earth latitude was  $0.6^\circ$  S and the solar phase angle was  $5.6^\circ$ .

<sup>a)</sup>Guest Observer, Mauna Kea Observatory, Institute of Astronomy, University of Hawaii, Honolulu, Hawaii.

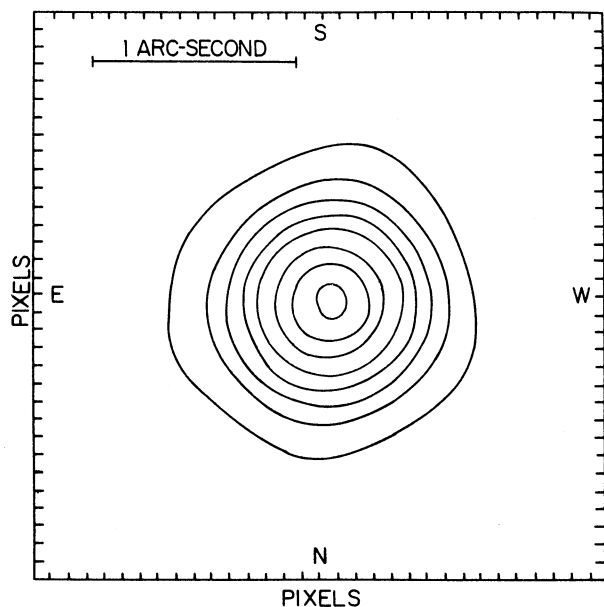


FIG. 2. Isophote contour map of Titan at 450 nm on 9 July 1980 obtained by speckle imaging. The central  $32 \times 32$ -pixel area from our  $128 \times 128$ -pixel frame is shown.

were digitized to 8-bit quantization (256 levels), with spatial filtering appropriate for a  $128 \times 128$ -pixel square grid for each video frame. 2000 frames were used for the white-light Titan data, 1000 for the 450-nm Titan data, and 200 for the  $\sigma$  Leo data. A contour plot of the reconstructed white-light Titan image is shown in Fig. 2. Figure 3 shows an east-west cut through the center of this image, along with a similar cut through the comparison source  $\sigma$  Leo. The latter represents the response of the imaging system to a point source (the "point spread

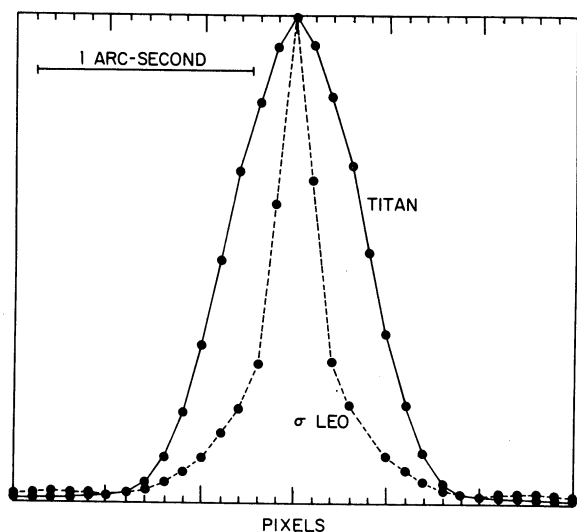


FIG. 3. East-west cuts through speckle images of Titan and star  $\sigma$  Leo at 450 nm scaled to the same central brightness.

function"), and demonstrates that the disk of Titan is resolved. Note that the image of Titan extends to a radius of about 7 pixels; roughly 150 pixels contribute to its two-dimensional, reconstructed image. The plate scale was determined by observations of known double stars to be  $0.0875 \pm 0.0017$  arcsec per pixel. Since Titan's distance from Earth at the time of our observations was 9.859 AU this scale corresponds to  $626 \pm 13$  km per pixel on Titan's image.

We could detect no significant departures from radial symmetry in the reconstructed Titan images and we therefore used the observed point spread function to determine the radius and limb darkening of the satellite in the following manner: We first generated trial limb-darkened disk intensity functions given by the power law

$$I(r)/I(0) = \mu^\alpha,$$

where  $\mu$ , the cosine of the zenith angle of the observer as seen from Titan, is given by

$$\mu = [1 - (r/R)^2]^{1/2},$$

where  $R$  is the radius of the satellite,  $r$  is the radius of the annulus contributing, and  $\alpha$  is the limb-darkening exponent. This simplified Minnaert function is appropriate for our observations, since the solar and terrestrial zenith angles differed by only  $5.6^\circ$ .

These trial limb-darkened disks were then convolved with the observed point spread function of the system (the  $\sigma$  Leo image), generating synthetic predictions of the observed Titan image for a range of values of  $R$  and  $\alpha$ . These synthesized Titan disks were then compared with the actual Titan image reconstructions out to a cut-off radius of 8 pixels, beyond which there is no significant image of the satellite. To do this, we first normal-

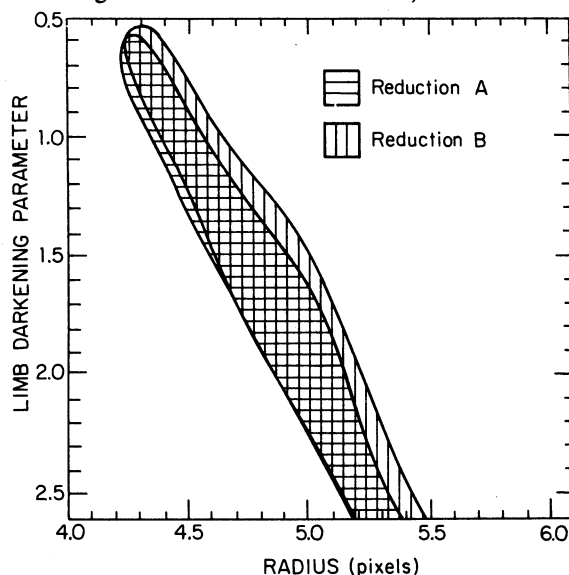


FIG. 4. Regions of parameter space for minimum variance between observed and synthetic data. The two shaded regions are for two different speckle reductions of the data. The white-light and 450-nm data have been combined.

ized the total intensities of the images to be compared, then summed the squared residuals over the two-dimensional image. This variance was plotted as a function of the model's radius ( $R$ ) and limb-darkening exponent ( $\alpha$ ). A two-dimensional contour plot of the variance vs  $R$  and  $\alpha$  showed a low trough with a fairly flat bottom and steep sides. The extent of the flat bottom is shown in Fig. 4 for one set of observed data, as reconstructed with two somewhat different pairs of speckle-reduction parameters (reductions A and B, respectively). These two reductions involved two different algorithms for eliminating a central "noise spike" artifact from processing images consisting of discrete photon events. There is some subjectivity involved in the best-choice parameters, but, as Fig. 4 demonstrates, the values of  $R$  and  $\alpha$  that define the trough are quite insensitive to the actual choice. The data plotted in Fig. 4 are the average of the white-light and filtered images, which are virtually identical; the parameters for Titan should, with good confidence, lie inside the area delineated.

#### IV. DISCUSSION

The image of  $\sigma$  Leo in Fig. 2 demonstrates the resolution that can be routinely obtained by speckle imaging; it is also an essential part of the reduction of the Titan data, serving as the point spread function calibration of the entire image-forming system (telescope optics, image-handling electronics, speckle-image reconstruction algorithms, etc.). The (radially symmetric) point spread function is well modeled by the sum of two terms:

$$I(r) \propto 4.2 \exp\left[-\left(\frac{r}{0.143}\right)^2\right] + 1.0 \exp\left[-\left(\frac{r}{0.42}\right)^2\right],$$

where  $r$  is the radius from the image center, in arcseconds.

The smaller-amplitude second term, probably a residual of the seeing disk as a result of inexact processing, has a full width of 0.84 arcsec. The seeing was estimated visually at the time of the observations to be about 1 arcsec. The first term has a full width of 0.29 arcsec and represents the resolution limit for these speckle-image reconstructions; it corresponds to a resolution limit of 3 pixels, close to the theoretical limit imposed by finite sampling of 2 pixels.

The relationship between the experimentally determined value of radius and limb-darkening exponent shown in Fig. 4 occurs because it is difficult to distinguish between the cases of strong limb darkening and large radius on the one hand, and weak limb darkening and small radius on the other. For a real planetary atmosphere it is unlikely that the limb-darkening exponent can exceed 1.3. According to Van de Hulst (1980), values of the Minnaert coefficient [ $k = (\alpha + 1)/2$ ] for the observed atmospheres range from 1.1 to 0.6 ( $\alpha = 1.2$ –0.2). It is difficult, moreover, to find parameters for homogeneous, semi-infinite atmosphere leading to large

values of  $\alpha$ . For example, for a single scattering albedo of 1.00 and a Henyey-Greenstein coefficient of 0.875, we obtain the strongest limb darkening in the tables of Van de Hulst (1980). For  $0.6 \leq \mu \leq 1.0$  the limb-darkening exponent from these data is  $\alpha = 1.26$ ; outside this range of  $\mu$  it is smaller.

We therefore adopt 0.6 as the lower limit to  $\alpha$ , based upon our measurements (Fig. 4), and 1.3 as the upper limit, based upon theoretical expectation. For these limits the corresponding radii of Titan at the cloud tops are  $2680 \pm 100$  km (for  $\alpha = 0.6$ ) and  $2900 \pm 100$  km (for  $\alpha = 1.3$ ).

Figure 5 shows a comparison of radial averages of the observed and synthetic data for  $\alpha = 0.9$ ,  $R = 2755$  km. The fit is typical for the permitted range of parameters. It is poor for the central 2 or 3 pixels without adopting large limb-darkening exponents, leading to a serious deterioration in the overall fit. There is, of course, no reason why the limb darkening should follow a simple power law. It is possible that we have observed enhanced backscatter from aerosols for small phase angles. This effect would not be detected by Voyager 1, which viewed Titan only at phase angles greater than  $20^\circ$ . If there is a central brightening of the satellite, however, it may be observed by Voyager 2.

Better data than those presented here were obtained from Pioneer-Saturn (Smith 1980) and Voyager 1 (Smith *et al.* 1981). The latter give a mean radius at the cloud

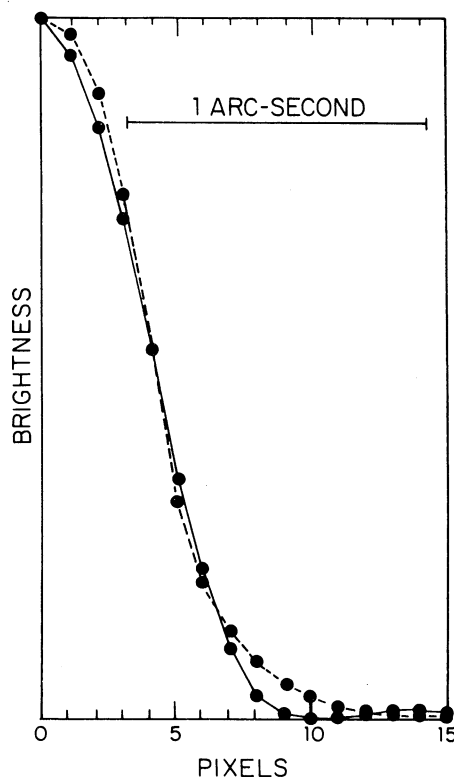


FIG. 5. Radial average of Titan image (solid curve) and of convolved synthetic disk with  $R = 4.4$  pixels (2755 km) and  $\alpha = 0.9$  (dashed curve).

top of  $2780 \pm 15$  km, which is compatible with our data for limb-darkening exponent of 0.98. The Pioneer-Saturn experiments measured both radius and limb darkening for phase angles greater than  $28^\circ$  (Tomasko 1980). According to Smith (1980), the average limb-darkening exponent in red light is 0.88 (range 0.38–1.0), and the mean radius is  $2840 \pm 25$  km. There are no discrepancies between our measurements and these spacecraft data, demonstrating some of the potential of speckle-imaging techniques.

There is no difficulty, in principle, in obtaining higher spatial resolution than we have achieved here. It could be doubled by using a grid of  $256 \times 256$  pixels of the time the image is digitized, and further improvements are probable with improved speckle-reduction techniques

now under development. Another factor of 2 can be gained by using a 4-m telescope. One can expect significant practical difficulties to arise, however, as the technique of speckle-image reconstruction is applied to images of higher resolution and lower light level.

We thank Robert Stachnik for determining the plate-scale calibration, Ron Tang for assistance in data reduction at Harvard University, W. T. K. Johnson and Dan Held for computation facilities at JPL, and Costas Papaliolios for continual advice and support. This work was supported in part by the NASA Planetary Astronomy Program under Grants No. NGL-22-007-228 to Harvard University and No. NAS 7-100 to the Jet Propulsion Laboratory, California Institute of Technology.

#### REFERENCES

- Knox, K. T., and Thompson, B. J. (1974). *Astrophys. J. Lett.* **193**, L45.  
 Nisenson, P., Stachnik, R., Papaliolios, C., and Horowitz, P. (1980).  
 In "Applications of Speckle Phenomena," edited by W. H. Carter  
 (Proc. Soc. Photo-Opt. Instrum. Eng. **243**, 88).  
 Smith, B. A., Soderblom, L. A., Johnson, T. V., Ingersoll, A. P., Ter-  
 rile, R. J., Collins, S. A., Shoemaker, E. M., Hunt, G. E., Masursky,  
 H., Carr, M. H., Davies, M. E., Cook, A. F., Boyce, J., Danielson,  
 G. E., Owen, T., Sagan, C., Beebe, R. F., Veverka, J., Strom, R. G.,  
 McCauley, J. F., Morrison, D., Briggs, G. A., and Suomi, V. E.  
 (1981). *Science* **212**, 163–190.  
 Smith, P. H. (1980). *J. Geophys. Res.* **85**, 5943–5947.  
 Tomasko, M. G. (1980). *J. Geophys. Res.* **85**, 5937–5942.  
 Van de Hulst, H. C. (1980). *Multiple Light Scattering* (Academic, New  
 York), Vol. 2.